



Identification of microplastics extracted from field soils amended with municipal biosolids

Maohui Chen^a, Brian Coleman^a, Liliana Gaburici^b, Daniel Prezgot^a, Zygmunt J. Jakubek^a, Branaavan Sivarajah^c, Jesse C. Vermaire^c, David R. Lapen^d, Jessica R. Velicogna^e, Juliska I. Princz^e, Jennifer F. Provencher^f, Shan Zou^{a,*}

^a Metrology Research Centre, National Research Council Canada, Ottawa, Ontario, Canada

^b Security and Disruptive Technologies Research Centre, National Research Council Canada, Ottawa, Ontario, Canada

^c Department of Geography and Environmental Studies, Carleton University, Ottawa, Ontario, Canada

^d Ottawa Research Development Centre, Science and Technology Branch, Agriculture and Agri-Food Canada, Ottawa, Ontario, Canada

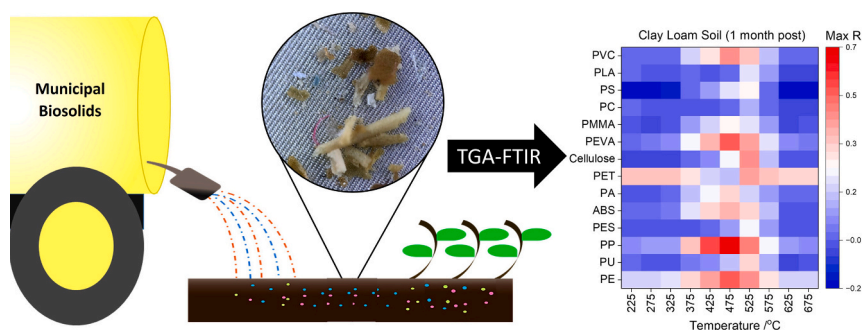
^e Biological Assessment and Standardization Section, Science and Technology Branch, Environment and Climate Change Canada, Ottawa, Ontario, Canada

^f National Wildlife Research Centre, Science and Technology Branch, Environment and Climate Change Canada, Ottawa, Ontario, Canada

HIGHLIGHTS

- Understanding the impact of municipal biosolids on microplastic contamination
- Developing reliable methods for microplastic extraction & characterization in soil
- Navigating challenges in identifying microplastics in soil samples
- Unraveling microplastic heterogeneity & fate in agricultural soil

GRAPHICAL ABSTRACT



ARTICLE INFO

Editor: Damià Barceló

Keywords:

Microplastics
Filtration
Agricultural soil
Municipal biosolids
Thermogravimetric analysis
FT-IR

ABSTRACT

Microplastic particles in arable soil are expected to impact the environment and potentially human health. The application of municipal biosolids (MBs) to agricultural land presents a further dilemma in that biosolids act as a fertilizer for crop growth, and a disposal pathway for wastewater treatment plants. They are also a direct path for emerging contaminants, such as microplastics to enter the terrestrial environment. Reliable methods are needed to identify and quantify microplastics, found in agricultural soils to determine how microplastics are being cycled in the terrestrial environment. In this study, we developed a method for extracting microplastics from soil, and characterized their composition and identity for particles sized 5 μm to 2 mm. Method development was initially completed using natural soils spiked with microplastics and MBs, followed by the analyses of soil sampled from an agricultural field where MBs were recently applied at a rate of 13 tons dw/ha. The procedures that used the spiked samples showed that microplastics can be reliably extracted from soil in a laboratory setting, and identified and semi-quantified by thermogravimetric analysis combined with Fourier-transform infrared spectroscopy (TGA-FTIR). However, when the same methods were applied to the soil samples collected from the agricultural

* Corresponding author.

E-mail address: Shan.Zou@nrc-cnrc.gc.ca (S. Zou).

<https://doi.org/10.1016/j.scitotenv.2023.168007>

Received 23 August 2023; Received in revised form 19 October 2023; Accepted 20 October 2023

Available online 21 October 2023

0048-9697/Crown Copyright © 2023 Published by Elsevier B.V. This is an open access article under the CC BY-NC-ND license (<http://creativecommons.org/licenses/by-nc-nd/4.0/>).

field, reproducibility became a challenge, as the number and type of microplastics changed even within the same soils (i.e., collected the same day from the same exact location). The variation in reproducibility observed between laboratory and field samples underscores the significant heterogeneity present in the environment. This heterogeneity, in turn, affects the identification and quantity of microplastics detected, a phenomenon observed even when comparing different fields within a single treatment regimen.

1. Introduction

Plastic pollution is of global concern, with terrestrial ecosystems estimated to receive up to forty times more plastic than aquatic systems (Kawecki and Nowack, 2019) an unsettling reminder of the need to better understand the life cycle and impact of plastics in terrestrial ecosystems. Microplastics (MPs) defined as a size of <5 mm (Bermúdez and Swarzenski, 2021) are of concern, and pose potential risks to animals as they are small enough to be ingested, and can disrupt biological processes and cause damage. The disintegration and degradation of MPs may yield nanoscale plastics (<1 μm), which may be more hazardous, given that the smaller size confers greater reactivity, but also permeation across cellular membranes (Wang et al., 2022; Kopatz et al., 2023; Li et al., 2023). This could subsequently lead to the uptake of nanoscale plastics by plants, the soil biome, and the potential for trophic transfer in the food web.

The cycling of plastics in the environment is an emerging research priority (Hu et al., 2022), and such research can be used to help mitigate plastic exposure to organisms of concern. The identification of MPs in the wastewater stream is of particular concern, as municipal biosolids (MBs, sludges) derived from wastewater treatment plants (WWTPs) are frequently amended to fields as a fertilizer (Nizzetto et al., 2016). This process can lead to elevated concentrations of MPs in soil systems, as most MPs are retained within the sludges (He et al., 2018; Crossman et al., 2020; Naderi Beni et al., 2023; Radford et al., 2023; Sivaraman et al., 2023). Currently, while there are some methods that have been used to assess microplastics in soil, there is a lack of standardized and harmonized methods that cover the range of terrestrial soil types often found in agricultural landscapes. Therefore, developing tools and testing methods for extracting and examining MPs from agricultural soils, including those enriched with municipal MBs is critical to better understand and address gaps related to characterizing the fate and effects of MPs in terrestrial systems.

While microplastics have been measured in a range of different environmental matrices, soil represents a more complex matrix than, for instance, water, snow, ice, or biota, which are more commonly examined with respect to MP concentrations. Therefore, in order to examine plastic pollution within a soil sample, there is a need to separate and remove both the mineral and organic components of the soil prior to being able to analyze any plastics that may be present. Several techniques have been tested to extract MPs from soil samples, and although a number of best practices (ASTM D8332-20, 2014; ASTM D8333-20, 2014) exist for the extraction of MPs from aquatic samples, techniques for soils are lacking; despite this gap, methods of analyses can be adapted from such established protocols. Primary treatment of soils includes manual sieving to concentrate and collect particles <5 mm (Bläsing and Amelung, 2018). Thereafter, the plastics must be separated from the soil's dense mineral content, or vice versa, the mineral content removed from the samples. Several methods for this step exist in the literature (He et al., 2021). One such technique is froth flotation, which was adapted from the recycling industry. Here, air bubbles are created in solution to carry the more hydrophobic particles to the surface of the solution, although the degree of success of this method is variable (Fraunholz, 2004; Alter, 2005; Imhof et al., 2012). Magnetic extraction has also been attempted, using functionalized iron nanoparticles to attract various plastics, although non-specific binding remains a recurring problem (Grbic et al., 2019; Rhein et al., 2019). Another proposed magnet based technique is vertical density gradient separation, as this

takes advantage of added colloidal ferromagnetic particles that are added to the mixture (Hu, 2014). A magnetic field is applied around the mixture, separating the particles from highest to lowest densities over a gradient. Other techniques include centrifugation and staining (Grause et al., 2022), electrostatic separation (Felsing et al., 2018; Silveira et al., 2018), elutriation (Kedzierski et al., 2016), and solvent extraction separation (Okoffo et al., 2020; La Nasa et al., 2021), each requiring highly specialized equipment.

The most common technique to separate and remove the soil mineral component is via a density separation technique (Nakajima et al., 2019) in which a concentrated salt solution is added to the sample to allow the MPs and organic soil components to float while the mineral component sinks. Various salt solutions have been tested, including sodium chloride (NaCl , 1.2 g/cm^3), calcium chloride (CaCl_2 , 1.01 g/cm^3), zinc chloride (ZnCl_2 , 1.5–1.7 g/cm^3), or sodium iodide (NaI , 1.8 g/cm^3) (Dekiff et al., 2014; Van Cauwenberghe et al., 2015; Kim et al., 2020; Bellasi et al., 2021; Mattsson et al., 2022). Salt solution approaches have shown some success (Han et al., 2019) with instances of being combined with canola oil in an attempt to improve the removal efficiency (Kononov et al., 2022). It should be noted these techniques are effective on the scale of MPs, but have limitations when considering nanoscale plastics (Wang et al., 2018). Various other types of oils have also been used, as the lipophilic properties of the plastics allow them to separate from the oils (Crichton et al., 2017; Lechthaler et al., 2020). Once the mineral components of the soil have been removed, the organic components can be subjected to chemical digestion using concentrated hydrogen peroxide (Nuelle et al., 2014; Li et al., 2019), nitric acid (Claessens et al., 2013), alkaline solutions (Foekema et al., 2013; Herrera et al., 2018) or through the use of a Fenton's reagent (Hurley et al., 2018; Liu et al., 2018; Frei et al., 2019). Should more digestion be required, enzymatic treatments are available to break down the proteins, pectins, and celluloses still mixed with the MPs (Cole et al., 2014; Mbachu et al., 2021; Palacios-Mateo et al., 2023; Toto et al., 2023). Thus, methods for the extraction of plastic particles from the soil matrix are varied in their approaches, each with respective advantages and disadvantages.

Once the MPs are extracted, a number of techniques can be used to quantify, identify, and characterize the recovered material. Some researchers have used visual techniques, such as Nile Red stains (Maes et al., 2017) or fluorescence microscopy (Grause et al., 2022) to quantify the particles. Various forms of chromatography have also been used to qualitatively and quantitatively identify the polymers, including High Temperature Gel Permeation Chromatography (HT-GPC) (Hintersteiner et al., 2015; Dümichen et al., 2017), Size Exclusion Chromatography (SEC) (Elert et al., 2017), and Pyrolysis Gas Chromatography Mass Spectrometry (Pyr GC-MS) (Fries et al., 2013), though these techniques all require extensive sample cleanup limiting bulk processing. Thermogravimetric Analysis (TGA) has seen an increase in usage as it is able to separate mixtures of MPs and quantify each component base, although like many of the chromatography techniques above, the sample is destroyed during analyses (Yu et al., 2019; Mansa and Zou, 2021; Fan et al., 2023). Coupling TGA with Fourier-transform infrared spectroscopy (FTIR) provides the ability to identify the MPs that are combusting, as most plastics will do so at different temperatures (Löder et al., 2015; Renner et al., 2017). Complementing TGA-FTIR with Raman spectroscopy can greatly improve the identification of MPs (Qiu et al., 2016; Cao et al., 2021; Nava et al., 2021; Sobhani et al., 2021; Dey, 2023). From these works, spectroscopic techniques have shown the greatest promise, especially due to their generally non-destructive

approaches.

This study focuses on the development and assessment of methodologies for detecting and characterizing microplastics in agricultural soils, with a specific emphasis on soils amended with municipal biosolids (MBs). The research endeavors to achieve the following objectives: (1) development and validation of an extraction method to effectively isolate microplastics from soil samples, with initial testing conducted using controlled, laboratory-prepared samples containing spiked microplastics and biosolids; (2) characterization of the composition and identity of microplastics, particularly those falling within the size range of 5 μm to 2 mm, present in the soil samples; and (3) comparative analysis of results obtained from laboratory-spiked samples and real-world field-collected samples, specifically from an agricultural site pre-MB application and at 1-month and 1-year post-application, to assess the reproducibility and reliability of the developed methods for samples collected in natural environmental conditions. It is only through a comprehensive examination of the extraction and characterization methods that we can have greater confidence in our analysis of the field soils, despite their inherent complexity.

2. Material and methods

2.1. Soils and biosolids

Two field-collected soils (sandy soil and clay loam soil), and raw municipal biosolids, sourced from a secondary level wastewater treatment facility with anaerobic digestion, were used throughout the study (Table 1). Briefly, the sandy soil was collected in 2017, dried and homogenized then used without further treatment. Pre-MB treated clay loam soil samples were collected in June 2021, with 1-month post collections occurring in July 2021, and the following May 2022. Five replicates were sampled from the field, taken within approximately 1 m of the original collection location.

The Ontario MBs applied to land were dewatered ('cake' consistency). For experimental purposes, the MB was applied to an area of an agricultural field at a rate of 13 tons dry weight/ha using a Kuhn Knight SLC 150 side discharge dry manure spreader. The MB was incorporated into the top 15 cm of soil immediately after application using a Sunflower Tillage-1435 disc harrow and secondary tillage seedbed preparation (performed soon after incorporation) was conducted using a Kuhn 122 series power tiller. The MBs in the incorporation zone of the soil were present as small aggregates (clods/clumps, Fig. S1). This resulted in localized spatial variability of MB aggregates over the field (Lapen et al., 2008; Edwards et al., 2009; Gottschall et al., 2010; Gottschall et al., 2012).

For experiments where MBs were manually added to the soils in the lab (i.e., not field-collected), the MBs were autoclaved (50 min steaming time, 121 $^{\circ}\text{C}$) and dried at 55 $^{\circ}\text{C}$; thereafter, they were ground with a soil grinder (Model SA-45, Gilson) with an attached 2 mm filter to remove larger particulates, including large debris. All soils were also ground and sieved, as described for the MBs prior to use. All samples were handled in glass or stainless-steel containers to minimize plastic contamination. Containers and instruments were pre-washed with MilliQ water (18.2 $\text{M}\Omega\cdot\text{cm}$ @ 25 $^{\circ}\text{C}$) prior to use. Samples were covered where possible using glass or aluminum foil.

Table 1
Mineral and organic properties of soils and MBs.

Soil type (region)	% sand	% silt	% clay	Total organic carbon (%)	Organic matter (%)	pH	CEC (cmol+/kg)
Sandy soil (Saskatchewan)	82	12	4	1.0	1.8	6.8	–
Clay loam soil; pre-MBs application (pre MB0–15 cm depth) (Ontario)	32	37	31	1.3	2.2	5.7	22
Clay loam soil; 1-month post MBs application (MB 0–15 cm depth) (Ontario)	35	36	29	2.1	3.5	5.7	24
MBs (Ontario)				25	4.3	7.3	98

2.2. Extraction methods

2.2.1. Extraction of PE from spiked sandy soil

The sandy soil was spiked with 0.33 wt% green fluorescent polyethylene beads (PE, 38–45 μm , Cospheric) by hand mixing the sample for 2 min. Three different density separation (flotation) solutions were assessed to determine their effectiveness for extracting MPs and organic component from the mineral component of the soil: CaCl_2 (1.32 g/cm^3 , Supelco, anhydrous granules), canola oil (Selection brand), and a NaI/NaCl mixture (1.5 g/cm^3 , both acquired from Sigma Aldrich, >99.5 %). The extraction process schematic is presented in Fig. 1. In this scenario, MBs were not amended into the soil.

Glass separators for density separation were created in-house (Nakajima et al., 2019). The PE was mixed with 50 g of sandy soil, and the mixture was added to the bottom separator with a stir bar. The flotation solution was then added until half of the upper apparatus was filled, and the mixture was stirred for 30 min. Thereafter, the solution sat undisturbed for 24 h in order to allow the denser particulates to fall out of the solution. After being allowed to rest, the density separator was closed, and the top layer was collected and filtered through 5 μm steel mesh filters (McMaster-Carr, washed with MilliQ water before being utilized). The filters were carefully rinsed with MilliQ water to collect all of the low-density material. The density separation process was repeated once more and combined with the previous collection of low-density material.

Following density separation, the Fenton's reagent was used to digest the collected material to remove organic matter from the sample. 0.05 M Fenton's reagent catalyst solution was freshly prepared with 7.5 g ferrous sulfate ($\text{FeSO}_4\cdot 7\text{H}_2\text{O}$, Sigma-Aldrich, $\geq 99\%$), 500 mL Milli-Q water, and 3 mL concentrated H_2SO_4 (ACP, 98 %). For an initial soil sample size of 50 g, 25 mL of the catalyst solution and 25 mL of 30 % hydrogen peroxide (Fisher Scientific) were slowly added over a period of 2 h to carry out the reaction, as the solution reacts quite vigorously. The solution was left overnight and then passed through a 5 μm steel mesh filter. Thereafter, a second density separation was performed on the filter cake to remove any trapped soil particulates that remained; this was then filtered one final time and dried overnight at 60 $^{\circ}\text{C}$.

2.2.2. Extraction of MPs from MB spiked clay loam soils

A second scenario included using the field-collected clay loam soil with no prior application of the MBs, to which a known concentration (0, 2 and 5 wt%) of MBs were added. At least 3 replicates of each were created, extracted, and analyzed. The same methodology (i.e., density separation and Fenton's digestion) was used to extract the MPs from the MB-spiked soils, although the density separation was only performed with NaI/NaCl. A sample of pure MBs was also tested in a similar fashion as a control (3 replicates). 50 g of soil was used for each amendment, and the resultant low-density material collected from the density separation was subjected to Fenton's reagent catalyst solution, followed by the slow addition of 30 % peroxide in a 1:1 (v/v) ratio.

Following the density separation and Fenton digestion, the filter cakes were subjected to enzymatic digestion to further remove extremely stable lignin and cellulose structures that were observed in the collected filter cakes. Consecutive enzymatic treatments of 1 mL pectinase L-40 (ASA) and 1 mL cellulase TXL (ASA) enzymes were

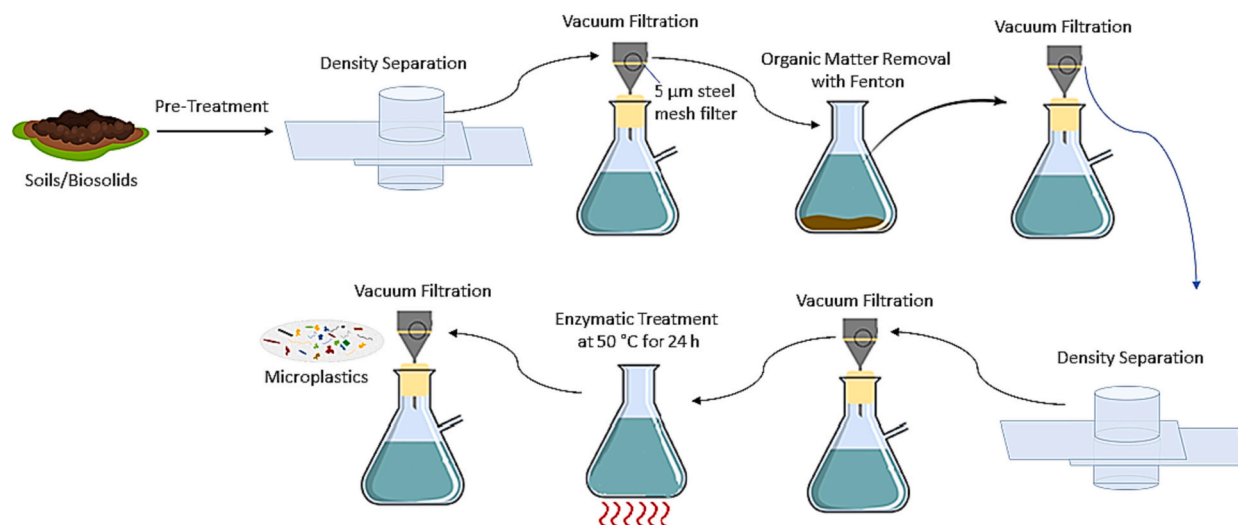


Fig. 1. Scheme depicting the process of extracting MPs from soil, soils amended with MBs, or MBs samples.

carried out in 25 mL 0.1 M NaAc (pH 5.0) at 50 °C for 24 h (Möller et al., 2022). After each enzyme treatment, the sample was filtered (5 μm stainless steel filter) and rinsed with Milli-Q water.

2.2.3. Extraction of MPs from field-collected clay loam soil post-MB application

The same extraction (separation and digestion) techniques were also applied to the field-collected clay loam soils, to which the MBs were applied to in the clay loam soil (as described in Section 2.1). Various initial sample sizes were tested, including 50 g, 750 g, and 2500 g, to determine if the initial sample size affected the number of MPs extracted. As large volumes were extremely difficult to work with (separators would become severely clogged with mud), the 750 g and 2500 g samples were processed and divided into 150 g samples for density separation. For the 750 g and 2500 g initial sample sizes, the digestion of the organic components involved Fenton's reagent catalyst solution being added to the separated and collected soil samples, followed by the slow introduction of 30 % hydrogen peroxide in a 1:1 (v/v) ratio. No enzymatic digestion was applied to the field-collected clay loam soils due to the lower amount of lignin and cellulose like materials in the filter cake after the Fenton's digestion compared to that extracted from the MBs (Section 2.2.2).

2.3. Identification and quantification of microplastics

Following density separation, digestion, and filtration, the collected materials were visually examined using an Echo Revolve Microscope (Bico, United States, 10× magnification, bright field imaging) to observe the presence of plastic particles. It should be noted that counting the number of particles was not within the scope of this work, as without confirming whether the particles observed were plastics or not, counting of particles would be misleading. Thus, no counting was performed in this study.

Thermogravimetric analysis (TGA) was then carried out using a Netzsch TG 209F1 Iris (TGA-MS-FTIR) system, by heating the sample from 40 °C to up to 1000 °C at a heating rate of 10 °C/min in an argon atmosphere (50 mL/min) and stabilized for 1 h. The TGA was coupled to an FTIR spectrometer (Bruker Tensor 27, Opus 8.5 software) to investigate in tandem, the sample composition (i.e., plastic chemical identification). Temperature and mass calibrations followed the manufacturer's recommended procedures. Typically, fifteen to twenty milligrams of dry sample were loaded into an empty aluminum oxide crucible that was pre-treated by annealing for about 30 s, ensuring a total mass loss of larger than 1 mg. The FTIR spectrum was collected at

about every 40 s which was determined by the operating software, with residence time in the transfer line of about 2.5 s in principle (although longer in reality). Thermograms were processed by excluding the mass loss below 200 °C due to the presence of water. Independently, more TGA analyses were also completed using a Netzsch Jupiter STA 449 F1 with the same heating rate and atmosphere. All TGA were processed with Proteus Analysis Software (version 8.0.2) and Smoothing (7th order) was applied to all the derived thermogravimetric curves (DTG).

From the TGA spectra, the "% PE in extracted sample" was determined based on the % mass change from the TGA spectrum between the regions of 400 and 500 °C, as this region is the area where most polymers are known to oxidize. The recovery efficiency of the initial PE spike was calculated using Eq. (1).

$$\% \text{efficiency} = \frac{(m_{\text{debris recovered from extraction}} * \% \text{PE recovered})}{m_{\text{initial PE spike}}} \quad (1)$$

The frequency range of raw FTIR data was cut from 600 to 4000 cm^{-1} and then smoothed with a selected method of "Concave Rubberband Correction" (e.g., 10 iterations and 64 baseline points) in OPUS. A Python 3 script in a Jupyter notebook (an open-source web-based interactive computing platform) was utilized to compare the spectra against a custom spectral library incorporating entries from the Open Specy (Cowger et al., 2021) and FLOPP/FLOPP-e (De Frond et al., 2021) open source FTIR spectral libraries of polymers. They were filtered such that only polymers with 10+ entries were included, leaving 14 possible search polymers (Table S1).

To perform spectral library matching, the spectral region of 750–3400 cm^{-1} (with the exclusion of the CO_2 regions of 600–750 cm^{-1} and 2240–2400 cm^{-1}) for the temperature range of 200–700 °C were selected for calculating Pearson's correlation coefficient (R) against each entry in the library. Prior to the matching, each spectrum was subject to Savitsky-Golay (SG) smoothing (3rd order) and adaptive smoothness penalized least squares (asPLS) baseline correction (Zhang et al., 2020). The resulting R-value, plastic ID, and temperature were compiled as a Polymer Identification (PID) matching heat-map in OriginPro 2021.

Raman analysis was performed using a Renishaw inVia confocal Raman microscope using a laser wavelength of 785 nm paired with a 1200 lines/mm grating. Measurements were made directly on the steel mesh filter, with an accumulation time of 10 s through a 20×/0.40 NA or 50×/0.75 NA objective in the spectral range of 720–1800 cm^{-1} using the SynchroScan feature. Data processing was performed using SG smoothing and as PLS baseline correction, as with the FTIR data, and spectra were likewise matched to a custom Raman library incorporating

entries from Open Specy and SLoPP / SLoPP-e libraries (Munno et al., 2020), with an R value >0.8 being considered a positive identification.

2.4. Statistical analysis

Standard uncertainties of various measurement results were calculated according to error propagation rules (GUM, 2008) by combining all recognized significant uncertainty contributions which included uncertainties of DTG peak area and TGA mass loss determination, initial and extracted material weighing, and, when applicable, material heterogeneity.

Multiple extractions were performed on the same clay loam 1-month post-biosolids application soil at various initial sample sizes. Mass fractions of MP in various extractions were compared against associated expanded uncertainties using the following formula

$\alpha = (x_1 - x_2)/2\sqrt{(u_1^2 + u_2^2)}$, where x_i and u_i are mass fraction and a corresponding uncertainty of i -th extraction and $k = 2$ expansion coefficient was used; $\alpha > 1$ indicates that the mass fractions are statistically different.

3. Results and discussion

3.1. Assessment of flotation solutions for density separation

The extraction (density separation and Fenton's digestion) methodology was tested using a field-collected sandy mineral soil that had been spiked with a known quantity (0.33 wt%) of green fluorescent polyethylene (0.92 g/cm³) (PE) microspheres. A sandy soil was used for these initial experiments, as opposed to the clay loam soils used in later experiments. MBs are commonly amended to sandy soils to increase organic matter, and the sandy soil we used also has an organic matter component comparable to the clay loams taken from the fields (Table 1). The method involved the use of a high-density solution to allow low density plastics and organic material to separate from the high-density mineral component of the soil. Three solutions were tested that were found to have good separation within the literature: CaCl₂, canola oil, and a NaI/NaCl mixture. CaCl₂ is dense enough to collect most common lower density polymers and is environmentally safe as a waste solution (Kononov et al., 2022). The oleophilic properties of canola oil allow for the separation of MPs away from the aqueous layer for collection (Radford et al., 2021). NaI/NaCl can create a very highly saturated solution, but must also be handled and disposed of accordingly due to its adverse effects on aquatic environments (Katsumi et al., 2022). The spiked sandy soil was subjected to all three solutions to evaluate and compare the efficacy of the density separation technique. After extraction, the resultant samples underwent Fenton digestion to remove any extraneous organic matter content from the sample; the soils contained approximately 2 % organic matter, comparable to the clay loam farm soils used in Sections 3.2 and 3.3. The resultant filtered material was collected and analyzed via TGA; results are provided in Fig. S2.

TGA is a process by which a sample of known mass is heated at a known rate. As the material in the sample reaches its oxidation temperature, the mass should change. The resulting mass loss will likely be associated with one component in the soil or multiple components that oxidize in a similar temperature range. The decomposition of PE is expected to occur at approximately (400–500) °C, which corresponds to the largest mass loss of this polymer in all TGA curves measured from all three extraction solutions (Fig. S2). Here the flotation solutions will be compared in terms of the purity of the PE sample (how much of the total mass loss in the TGA comes from the PE), and the recovery efficiency of the initial PE spike (the mass of debris extracted divided by the initial mass of the PE spike) (Table 2).

Here the “% PE in extracted sample” is based on the % mass change from the TGA spectrum between the regions of 400 to 500 °C, as this region is the area where most polymers are known to oxidize. The

Table 2

Comparison of PE extraction from clay loam soil by density separation (flotation) in various solutions (the numbers shown are the mean value ± corresponding standard uncertainty).

Flotation solution	% PE in extracted sample	Recovery efficiency of initial PE spike (%)
CaCl ₂	44 ± 14	42 ± 25
Canola oil	70 ± 6	52 ± 10
NaI/NaCl	88 ± 5	54 ± 10

recovery efficiency of the initial PE spike was previously calculated using Eq. (1).

CaCl₂ was tested first, as it has a higher density than most common polymers, and is quite safe to use, both for humans and the environment. Unfortunately, CaCl₂ demonstrated large variability between samples, as the % PE in the final sample over multiple runs varied drastically (44 ± 14)%. It was also only able to collect less than half of the initial PE spike (42 ± 25)%, likely owing to its comparatively low overall density.

Next, Canola oil was tested as a flotation solution. While it was found to improve upon CaCl₂ in terms of % PE in the extracted sample (70 ± 6)% and recovery efficiency of the initial spike (52 ± 10)%, far too much of the sample is comprised of mineral and organic components from the soil, rather than only MPs. The recovery efficiency also shows half of the initial PE spike was not extracted, meaning too much PE remained unextracted in the process.

The final flotation solution was a mixture of NaI/NaCl. This mixture is able to attain the highest density solution of those tested. The use of the NaI/NaCl solution demonstrated the highest purity of PE, i.e. (88 ± 5)%, extracted from the soil, with the greatest recovery efficiency of the initial PE spike i.e., (54 ± 10)%. Full recovery was likely not attained here as the plastics can remain trapped within or adhered to the soil mineral content, and thus are weighed down (Sivarajah et al., 2023). Nevertheless, the high density of the NaI/NaCl solution likely plays a major role here, as the low-density PE will have an even greater propensity to float in such a solution.

As there are many polymers that have density greater than that of PE, NaI/NaCl was also applied to the extraction of PTFE (2.2 g/cm³) from the sandy soil to determine the effectiveness of the process for high density polymers, as soil mixtures are likely to contain more than just low-density PE. Although some PTFE was recoverable (Table S2), a lower effective recovery rate occurred relative to the low-density polymer (PE). As lower density solutions such as CaCl₂ and canola oil struggled with PE, it is unlikely they would achieve better results than the NaI/NaCl. Therefore, NaI/NaCl was selected as the main flotation solution for the subsequent tests.

3.2. Verification of TGA-FTIR analyses in lab-spiked MB-clay loam soil

Following a comparison of flotation solutions using the sandy soil, the optimal solution (NaI/NaCl) was used for the extraction of MPs from the clay loam soils (50 g) that were lab-spiked with known amounts of MB (0, 2, and 5 wt%). The MPs were extracted using the NaI/NaCl density separation (flotation) solution and Fenton digestion to remove the organic matter. However, due to the presence of cellulose or cellulose-like content in MB, this study goes beyond the normal protocols found in the literature to include an enzymatic digestion step to further break down the cellulose in the MB control and MB spiked samples (Möller et al., 2022). While a Fenton reagent performs admirably at breaking down most organic material, the application of first a pectinase and then a cellulase allows for the targeted breakdown of some of the sturdier linkages found in organic material. By breaking the fibers down further and further, MPs can be further dislodged from any accumulations of organic material that the MPs may adhere to, improving the extraction yield.

Once the soil samples underwent both chemical and enzymatic

digestion, the extracted materials were filtered and collected and plastics-like particles (fiber, pellets, and fragments) were observed under the microscope (Fig. 2). Larger brown pieces were manually selected under the microscope and confirmed to be cellulose-like material by Raman and FTIR (Fig. S4).

With TGA analysis, a mass loss corresponding to both cellulose (at $\sim 200\text{--}400$ °C) and the MPs (at $\sim 400\text{--}500$ °C) was observed (Fig. 3). When examining the Derivative Thermogravimetry curve (DTG), a much clearer separation between these two peaks can be seen. Gauss peak fittings were carried out on the spectra to build a calibration curve encompassing 0 wt%, 2 wt%, and 5 wt% MB added to the 50 g clay loam soils, respectively. Specifically, two peaks around 360 and 460 °C, respectively (see Fig. 3a), were fitted and areas under the specific peaks were calculated, to compare the DTG curve area against the MB concentration (Fig. 3b and Table S3).

The calibration curve of the area corresponding to MPs with cellulose in Fig. 3b showed that MPs were found in the highest concentration within the 5 g MB sample, with a subsequent decrease in MP content as the percentage of MB in the clay loam soil decreased. When no MB was added to the clay loam sample (0 wt%, 50 g), the concentration of MP was low, though still detectable in the control clay loam soil (3 replicates). The MP detected in the extracted samples from 2 wt% MB spiked one (in 50 g soil) was low as well, which showed a similar area number to the 0 wt% one. Therefore, the vast majority of measured MP from the amended soils (in 50 g soils) came from the spike of MBs.

2D wavelength versus temperature FTIR maps were created from the TGA-FTIR data to identify functional groups of interest (e.g., methylene, ketone, and alkenes) with varying temperatures using a customized macro in Fiji (ImageJ 1.53 t, Fig. 4), rather than the traditional absorbance versus wavelength FTIR spectrum and 3D FTIR spectra against temperature in Fig. S5. The 2D FTIR map (see Fig. 4) highlights the types of common functional groups that can be found during the pyrolysis of MPs, such as --OH (broad peak around 3300 cm^{-1}), C--H (around 2950 cm^{-1} and 2850 cm^{-1}), C=O (around 1720 cm^{-1}), carbon monoxide and carbon dioxide, mainly generated from the decomposition of plastics.

To efficiently identify the types of plastics in the collected debris, we developed a novel method for interpreting the results, compiling them in the form of a Polymer Identification (PID) heat-map (see more details in Section 2.3). Herein, the identification of the strongest match appears in red (i.e., Max R), and those with a poor-to-no-match in blue (Fig. 5). From the PID, PET, PP, PE, and acrylonitrile butadiene styrene (ABS) show strong R matches, suggesting they are found in the mixtures.

It should be noted that, generally, an R value of larger than 0.7 is considered as a positive match of polymer type for FTIR spectral comparison (Buhl-Mortensen and Buhl-Mortensen, 2017). In the “Open Specy Guide Lines”, “if no matches are >0.3 , the material may require

additional processing or may not exist in the Open Specy library” (Cowger et al., 2021). The IR spectra attained during the pyrolysis process of TGA are in the gas phase, as opposed to the room temperature spectra found in the two open-source libraries. For our studies of polymer identification, we considered an R value >0.3 as a positive match. In the MBs (Fig. 5a), polyethylene terephthalate (PET), polyethylene (PE) and polypropylene (PP) were found with R values >0.3 , suggesting their presence in the sample.

To further develop the PID mapping method, TGA-FTIR measurements of commercially available plastics (used as control experiments) were applied (commercial PE, PP, and PET in Fig. S6a-c), together with the extracted sample from 5 g spiked MB in 750 g clay loam (Fig. S6d) to verify the matching approach. In Fig. S6a-c, the maximal R values were clearly observed for the PE (~ 0.6), PP (~ 0.8), and PET (0.4), respectively. For the sample spiked with 5 g of MB (0.7 % in 750 g soil), the polymers with higher matching R values indicated the existence of PE, PP, and PET, demonstrating consistency in detection across samples with the same source of MB (Fig. S6d). The results from this initial study indicate that MPs can be quantified in the sense of total plastics by TGA, and the polymer types can be identified by the PID heat map from soil samples spiked with MBs using TGA-FTIR. This indicates they should be effective tools for use with field samples.

3.3. Analysis of clay loam soil samples treated with an unknown quantity of MBs

With a toolset in place, analysis of MB-amended clay loam soils was carried out using the extraction protocol from the lab-spiked clay loam samples. Field samples were collected prior to MB application, 1-month and 1-year post-application, each in a sample size of 50 g.

Each of these extracted samples was analyzed using TGA (Fig. 6a) and the representative optical images are shown in Fig. 6b-d. Of the three, the 1-month post-application sample was found to have the greatest mass percentage of MPs (16 %, Table S4). The pre-treated (14 %) and 1-year post-application (10 %) both had lower quantities of MPs, suggesting that after 1 year, the number of MPs in the soil is reduced within the surface depth measured in this study. FTIR was run in tandem with TGA, with the IR signals of some plastics (PET) being found with relatively high confidence in the plastic ID heat-map (Fig. 7). Research is still ongoing to correlate the IR spectra in the gas phase at varied temperatures for a given ID of plastics. A collection of common plastics will be tested on TGA-FTIR and compiled into a self-built library, with aging and size factors taken into consideration. However, for the purpose of this study, three top-hit plastics (PET, PE, and PP) were tested and the resulting plastic ID heat-map shown in Fig. S6.

Raman microscopy was performed on a subset of the filtered 1-

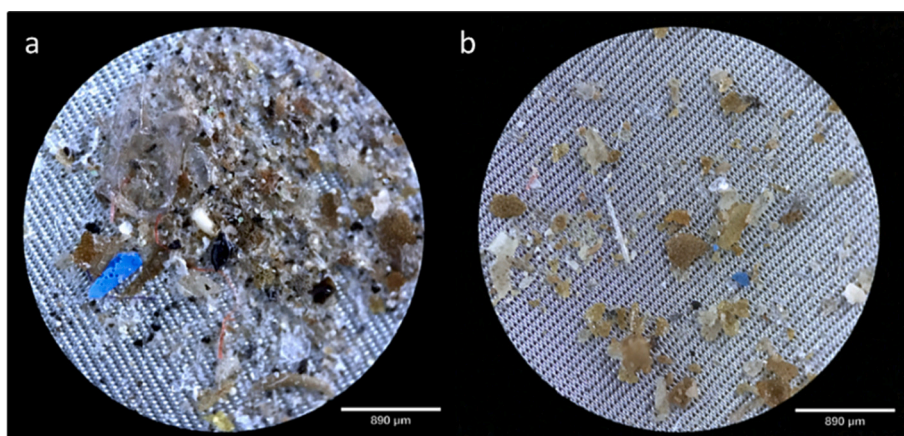


Fig. 2. Plastic debris extracted from a) clay loam soil lab-spiked with municipal biosolids (5 wt%) and b) pure municipal biosolids (5 g sample). 0 wt% and 2 wt% MB in 50 g clay loam is shown in Fig. S3. Scale bars are 890 μm .

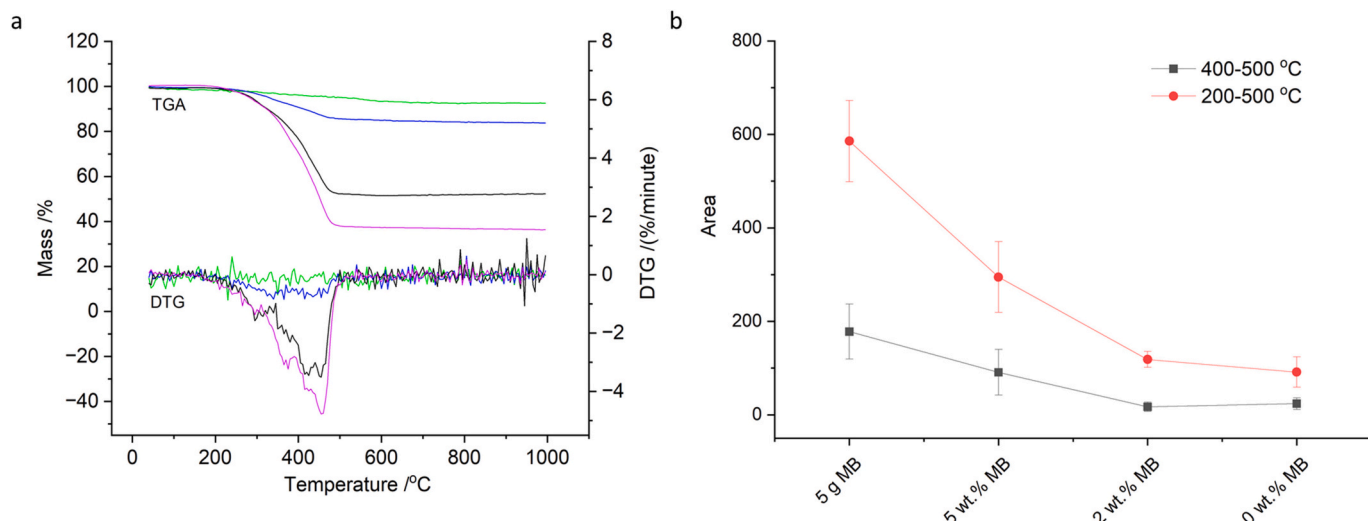


Fig. 3. (a) TGA (left axis) and DTG (right axis) curves depicting 0 wt% (green), 2 wt% (blue), 5 wt% (black) MB addition to 50 g clay loam soil and 5 g MB (purple). (b) Representative calibration curves showing the areas from Gauss peak fitting in OriginPro 2021, corresponding to the peak at (400–500) °C, black; and the peak at (200–500) °C, red (including the cellulose). The error bar represents the standard uncertainty from four (4) samples for 5 g biosolid, four (4) samples for 5 wt%, three (3) samples for 2 wt% and three (3) samples for 0 wt%.

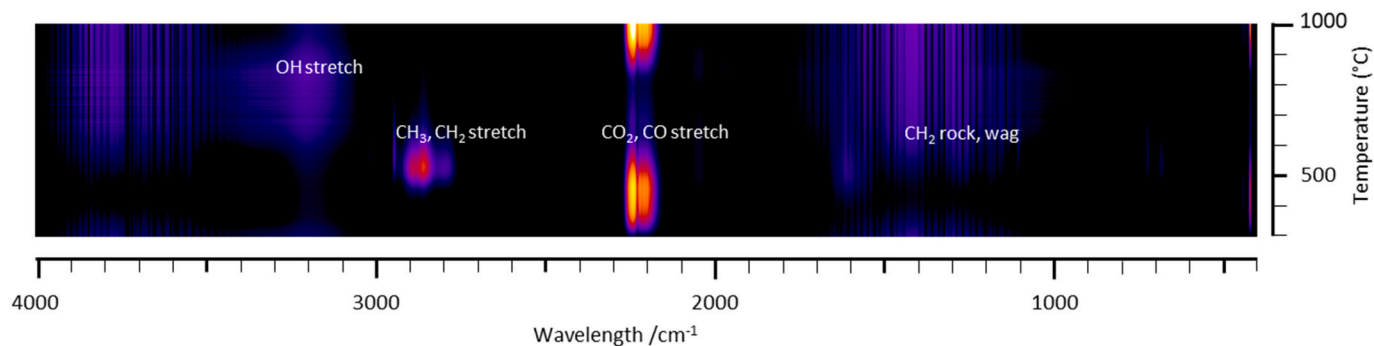


Fig. 4. Representative FTIR 2D map of municipal biosolids. A total of 304 FTIR spectra were collected from the thermal cycle from 300 to 1000 °C at a heating rate of 10 °C/min. The absorption bands are highlighted and can be used to identify the functional group.

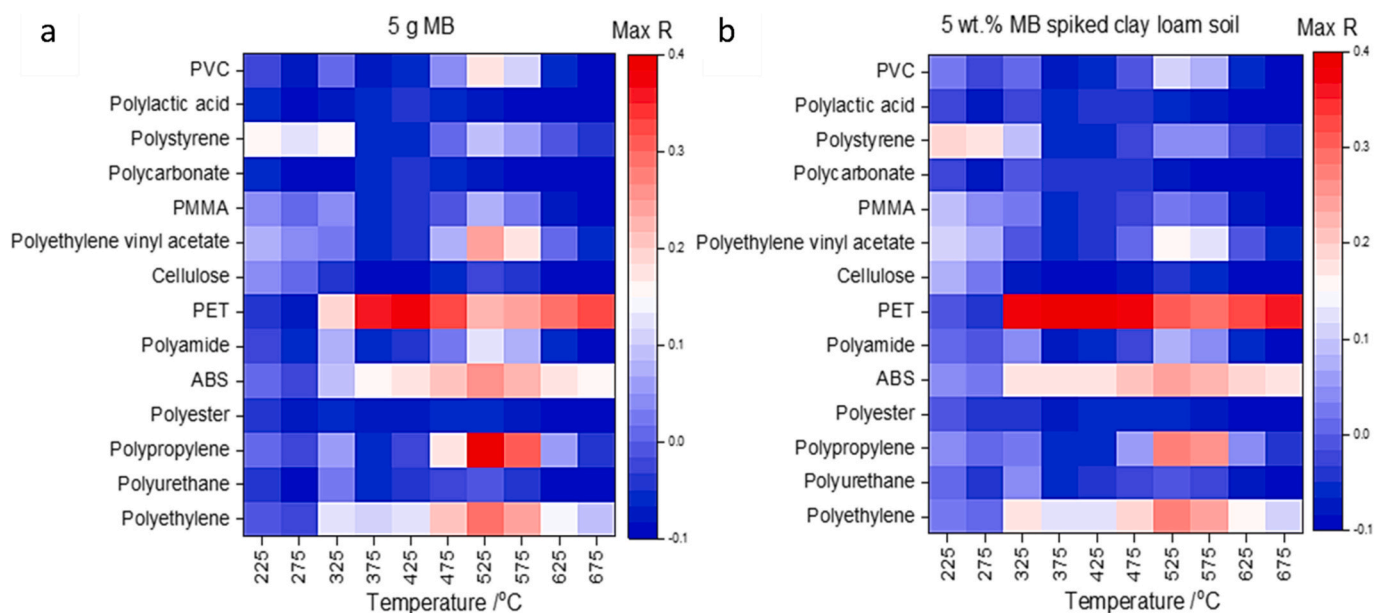


Fig. 5. PID heat maps based on FTIR spectra for a) MB only and b) 5 wt% MB spiked into 50 g clay loam soil.

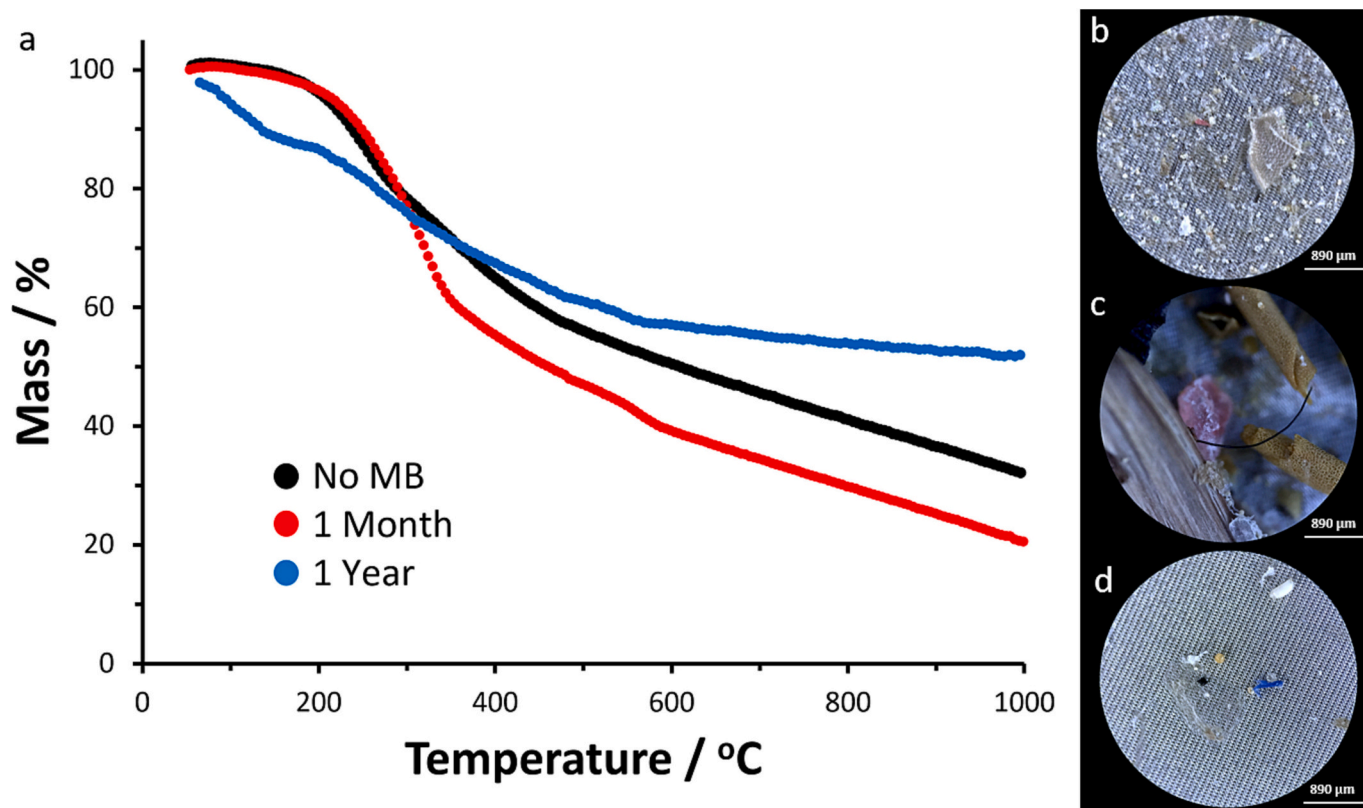


Fig. 6. a) TGA plot comparing clay loam soils collected from an agricultural field before and after MB treatment (each in a sample size of 50 g) with microscope images of the particles for b) pre-MB application, c) 1-month post-MB application, and d) 1-year post-MB application.

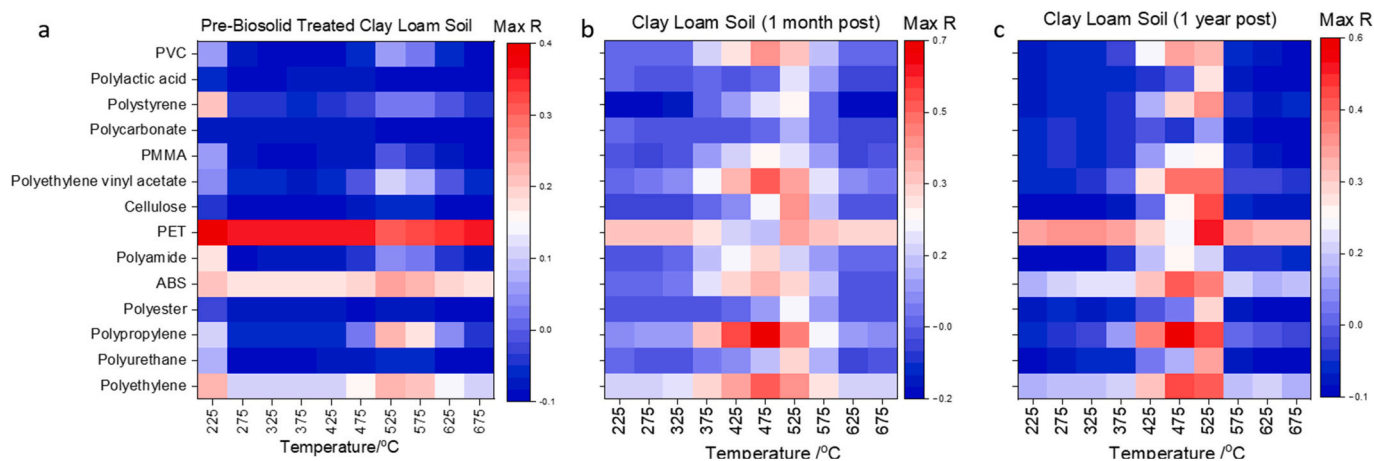


Fig. 7. PID heat maps based on FTIR spectra for 750 g a) pre-MB treated, b) one month, and c) one-year post-MB treatment clay loam soils.

month and 1-year post-application samples to confirm the presence and identity of microplastics. Significant background fluorescence and low signal-to-noise obfuscated the Raman scattering of most particles, making identification difficult by this method. This also highlights the importance of quantification and identification for bulk MPs using our TGA-FTIR analysis method. Nevertheless, expected plastics such as PE and PP were confirmed to be present as well as remaining cellulosic material (Fig. S7).

Additional extractions were performed on further samples of the 1-month post-application treatment (Fig. 8). This included performing three extractions at 50 g initial sample sizes, two extractions with a 750 g initial sample size, and one further extraction at a 2500 g sample size. Analysis of the results, as described above, showed that with the limited

number of extractions the mass fractions of MP in the extractions were not statistically different between the sample sizes (50 g vs. 750 g), but different within the same sample size (e.g., 50 g A vs. B vs. C), see Table 3. Since the scalability of the extraction process to sample sizes >750 g was found near unfeasible, only one large sample size extraction (2500 g) was selected. Based on the analysis we concluded that the material heterogeneity rather than sample size was responsible for the mass fraction of MP variation.

The results from the analysis of the field-collected soils indicated that the MP extraction efficiency (mass of MPs extracted divided by initial soil mass) was quite low for the given soil samples (0.05 mg MP/g soil), especially compared with the efficiency of the extraction on the PE ((88 ± 5) %) previously performed. The Gaussian multiple peaks fitting of the

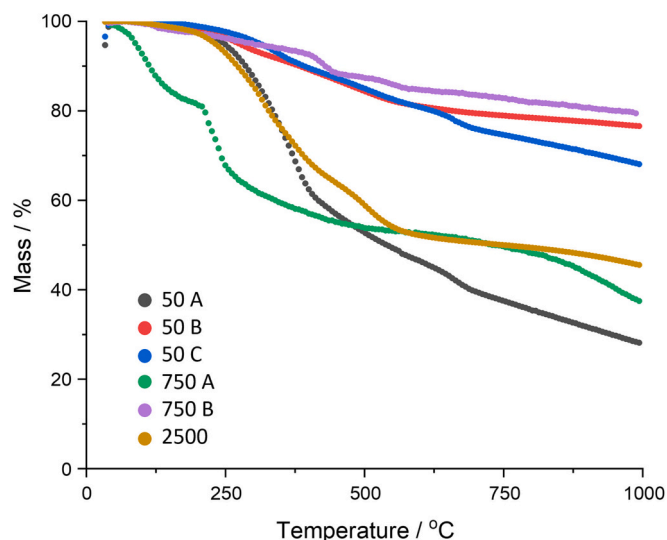


Fig. 8. Comparison of extractions performed on clay loam soil 1-month post-biosolids application at various initial sample sizes. Numbers in legend represent the initial sample size of soil extracted (see also Table 3): Three 50 g, two 750 g, and one 2500 g samples.

Table 3

Comparison of multiple extractions performed on clay loam soil 1-month post-biosolids application (the numbers shown are the quantity value \pm corresponding standard uncertainty).

Sample	Mass of debris collected (mg)	TGA mass fraction loss (in %) corresponding to MP (400–500) °C	Mass of MP in debris (mg)	Mass fraction of MP in soil (mg/kg)
50 g A	0.41 \pm 0.03	8.3 \pm 0.37	0.034 \pm 0.003	0.68 \pm 0.06
50 g B	1.91 \pm 0.03	4.8 \pm 0.22	0.092 \pm 0.004	1.83 \pm 0.09
50 g C	1.90 \pm 0.03	5.3 \pm 0.24	0.100 \pm 0.005	2.01 \pm 0.10
750 g A	100 \pm 12	3.1 \pm 0.14	3.1 \pm 0.4	4.15 \pm 0.53
750 g B	660 \pm 12	5.3 \pm 0.24	35.2 \pm 1.7	47.0 \pm 2.3
2500 g	180 \pm 12	10.3 \pm 0.46	18.5 \pm 1.5	7.41 \pm 0.60

DTG curve within the (400–500) °C range yielded a fitted area ranging from 33.2 to 102.5 (as shown in Table S5) when analyzing soils of 50 g to 2500 g from the 1-month post-MB application. These values correspond to the presence of 1 g to 2.5 g of MBs in the clay loam soil, determined based on the calibration curve (Fig. 3b). In a control experiment, 750 g of clay loam soil was added with 0.7 wt% MBs (equivalent to 5 g of MBs, Fig. S6d). The TGA-FTIR analysis revealed the identification of plastics similar to those observed in pure MBs and in soil spiked with 5 wt% MBs (Fig. 5).

Upon applying Gaussian fitting to the DTG curve within the (400–500) °C range for the 750 g soil samples from the 1-month post-MB treatment, an area value of 33.2 was obtained (for the 750 B in Fig. 8, also see Table S5). Notably, this area value concurs with the outcome derived from the analysis of the 750 g soil sample spiked with 5 g of MBs, which yielded an area value of 52. This outcome underscores the influence of the quantity of soil samples analyzed in determining the concentration of MPs in the 1-month post-MB treated clay loam soil. Nonetheless, the results consistently indicate that approximately (0.5–5) wt% of MBs persisted in the clay soils, with the range reflecting the analysis of samples ranging from 50 g to 2500 g.

As the extraction method was shown to recover a large percentage of

the MPs in the spiked soil samples, it can be postulated that the number of MPs present in the field-collected soil (with and without biosolids) is so low, that even a small grouping of MPs can vastly change the results. This large variation (from 0.68 mg/kg to 47 mg/kg) is likely due to the natural heterogeneous distribution of the MBs (cake) aggregates to the field via the commercial scale application and biosolids-soil incorporation process (Gottschall et al., 2012), which can create pockets of low and high concentrations of MB derived constituents in the field. This makes sense when one considers the method for MB distribution, in which a manure spreader releases the waste solution in an arc from a central nozzle on the holding tank, inevitably gaps on the field where MBs will not be dispersed. The MBs that are distributed will also be dispersed on the surface of the soil, where it is much more easily dislodged than if it was introduced deeper into the soil. This can be visualized further when we compare the mass of the MPs extracted compared to the initial mass of soil, where on the whole more MPs were found in the larger initial soil samples (Tables 3 and S5). As these encompass a larger sampling size that would more readily capture biosolid aggregates in the sample. This is important to consider within the context of what soil invertebrates may be exposed to via these types of applications.

Moreover, the field soil environment is dynamic in terms of the factors that redistribute (i.e., water/wind drivers and soil management practices like tillage), sequester, and transform MPs over time (Crossman et al., 2020; Ding et al., 2020). For example, soil characteristics, such as soil density and depth, have been shown to increase the retention of MPs in soil, as MPs that have been inserted deeper into the soil are retained longer than those closer to the surface where weathering and human activity are more likely to disturb the soil. (Crossman et al., 2020). Also, the presence and activity of soilorganisms also influence the retention of MPs, as arthropods (Maaß et al., 2017), fungi (Wick et al., 2007), and earthworms (Rillig et al., 2017) have all shown the ability to actively transport MPs through the soil or create pores to facilitate MP movement through the soil environment. Given the heterogeneous structure and nature of soils in the field, sampling strategies must be sufficiently robust to capture the distribution of the MPs within and across the treatment field; this includes being able to capture the spatial variability of MB applied to soil, but also repeated sampling over several time points, as soil is subject to rain, wind, and animal activity throughout the seasons.

4. Conclusions

A great number of tools will be necessary to not only analyze MP pollution within terrestrial systems, but also characterize the risk to organisms within these systems, crops being produced, and to human consumption. This study has shown that MPs within soil and municipal biosolids can be collected, identified, and quantified using readily available techniques; however, more effort is required on sample design and collection, given the natural heterogeneity of soils, heterogeneity in amendment practices (e.g., biosolids application), and variability in the occurrence of pollutants. The MP spiking experiments demonstrate the efficacy of density separation and organic enzymatic digestion techniques that allow for the collection of MPs with reasonable recovery. The TGA has shown that a mixture of MPs can be quantified within a field sample, with FTIR being able to identify the different polymers. For the clay loam field soils, challenges with repeatability occurred between samples, even when collected within a few meters of sampling. This is a reflection of the natural spatial heterogeneity in the distribution of MBs over the field as a result of commercial scale land application practices. Therefore, sampling designs will be critical as we continue to understand plastic cycling in the terrestrial environment, and more specifically in agricultural landscapes where soil amendments are common. In addition to sampling, both characterization and recovery of spiked samples will be integral to the chemical analysis of environmentally-derived samples. Characterization libraries must also be expanded to take into account

changes to the MPs that will occur in the environment through either anthropogenic or natural processes. For example, wastewater and biosolids are subject to a variety of treatment processes (e.g., aerobic and anaerobic digestion, microbial or enzymatic processes, etc.) that will influence the type and quantity of MPs that will accumulate within. Moreover, natural weathering processes that MPs become exposed to will also affect their spectra in IR compared with pristine samples (De Frond et al., 2021), or their overall absorptive and solubility properties (Ho et al., 2020; Aghilinasrollahabadi et al., 2021; Yang et al., 2021).

This study helps lay out some of the issues studying MPs in complex soil matrices, but by carrying out this work, we can suggest improvements in a number of areas that will help minimize constraints on MP characterization. Firstly, due to spatial variability issues associated with commercial scale land application practices, it's crucial to invest in standardized, robust sampling protocols to ensure representation of MBs (and MPs) distributed in a field environment. Secondly, we recommend further exploration and refinement of density separation and enzymatic digestion methods for efficient MP collection in environmental analysis. These techniques have shown promising recovery rates, particularly targeting plastics. The enzymatic digestion in particular could lead to improvements in extraction efficiency, as it has been designed to break down the organic material in a top-down manner. Thirdly, TGA and FTIR proved valuable for quantifying and identifying MPs in field samples. To account for environmental changes, it's important to expand characterization libraries. While these methods can be time-consuming, they provide concrete data, especially when coupled with computer-assisted analysis algorithms, making them a valuable toolkit for MP analysis in soil and biosolid samples. Moreover, enhancing MP analysis with diverse biosolid, soil, and MP types can also improve our understanding of the fate and transport of MPs resulting from land application practices. Finally, to gain a comprehensive grasp of plastic pollution in soils, long-term monitoring should be considered. This approach should encompass not only spatial variations but also integrate elements such as depth and time into sample collection and analysis protocols. This holistic perspective helps build a more complete picture of the issue over time. This together, with balancing efforts to improve sample collection design, within and across field samples, with time, and integrating elements such as depth and time, will allow the true nature of plastics pollution in soils to be revealed.

CRedit authorship contribution statement

BC, MC, LG, JRV, and JIP performed measurements; DP and ZJ created the macros and BC, DP, MC, ZJ, and SZ analyzed the data; BS, DL, JFP, JIP, JCV, and JRV designed field treatment and collected samples; BC, MC and SZ wrote the paper with input from the co-authors; DL, JFP, JIP, and SZ secured funding. All co-authors reviewed and edited the paper for clarity.

Declaration of competing interest

The authors declare that they have no known competing financial interests or personal relationships that could have appeared to influence the work reported in this paper.

Data availability

All data generated or analyzed during this study are included in the paper and will be available upon request.

Acknowledgments

The authors appreciate the Ocean Program at the National Research Council Canada (NRC) and the Advancing a Circular Plastics Economy for Canada Program from the Government of Canada for financial support.

Appendix A. Supplementary data

Supplementary data to this article can be found online at <https://doi.org/10.1016/j.scitotenv.2023.168007>.

References

- Aghilinasrollahabadi, K., Salehi, M., Fujiwara, T., 2021. Investigate the influence of microplastics weathering on their heavy metals uptake in stormwater. *J. Hazard. Mater.* 408, 124439 <https://doi.org/10.1016/j.jhazmat.2020.124439>.
- Alter, H., 2005. The recovery of plastics from waste with reference to froth flotation. *Resour. Conserv. Recycl.* 43 (2), 119–132. <https://doi.org/10.1016/j.resconrec.2004.05.003>.
- ASTM D8332-20, 2014. Standard Practice for Collection of Water Samples with High, Medium, or Low Suspended Solids for Identification and Quantification of Microplastic Particles and Fibers. ASTM International, West Conshohocken, PA. <https://doi.org/10.1520/D8332-20>.
- ASTM D8333-20, 2014. Standard Practice for Preparation of Water Samples with High, Medium, or Low Suspended Solids for Identification and Quantification of Microplastic Particles and Fibers Using Raman Spectroscopy, IR Spectroscopy, or Pyrolysis-GC/MS. ASTM International, West Conshohocken, PA. <https://doi.org/10.1520/D8333-20>.
- Bellasi, A., Binda, G., Pozzi, A., Boldrocchi, G., Bettinetti, R., 2021. The extraction of microplastics from sediments: an overview of existing methods and the proposal of a new and green alternative. *Chemosphere* 278, 130357. <https://doi.org/10.1016/j.chemosphere.2021.130357>.
- Bermúdez, J.R., Swarzenski, P.W., 2021. A microplastic size classification scheme aligned with universal plankton survey methods. *MethodsX* 8, 101516. <https://doi.org/10.1016/j.mex.2021.101516>.
- Bläsing, M., Amelung, W., 2018. Plastics in soil: analytical methods and possible sources. *Sci. Total Environ.* 612, 422–435. <https://doi.org/10.1016/j.scitotenv.2017.08.086>.
- Buhl-Mortensen, L., Buhl-Mortensen, P., 2017. Marine litter in the Nordic Seas: distribution composition and abundance. *Mar. Pollut. Bull.* 125 (1–2), 260–270. <https://doi.org/10.1016/j.marpolbul.2017.08.048>.
- Cao, J., Zhao, X., Gao, X., Zhang, L., Hu, Q., Siddique, K.H.M., 2021. Extraction and identification methods of microplastics and nanoplastics in agricultural soil: a review. *J. Environ. Manag.* 294, 112997 <https://doi.org/10.1016/j.jenvman.2021.112997>.
- Claessens, M., Van Cauwenberghe, L., Vandegheuchte, M.B., Janssen, C.R., 2013. New techniques for the detection of microplastics in sediments and field collected organisms. *Mar. Pollut. Bull.* 70 (1), 227–233. <https://doi.org/10.1016/j.marpolbul.2013.03.009>.
- Cole, M., Webb, H., Lindeque, P.K., Fileman, E.S., Halsband, C., Galloway, T.S., 2014. Isolation of microplastics in biota-rich seawater samples and marine organisms. *Sci. Rep.* 4 (1), 4528. <https://doi.org/10.1038/srep04528>.
- Cowger, W., Steinmetz, Z., Gray, A., Munno, K., Lynch, J., Hapich, H., Primpke, S., De Frond, H., Rochman, C., Herodotou, O., 2021. Microplastic spectral classification needs an open source community: open specy to the rescue! *Anal. Chem.* 93 (21), 7543–7548. <https://doi.org/10.1021/acs.analchem.1c00123>.
- Crichton, E.M., Noël, M., Gies, E.A., Ross, P.S., 2017. A novel, density-independent and FTIR-compatible approach for the rapid extraction of microplastics from aquatic sediments. *Anal. Methods* 9 (9), 1419–1428. <https://doi.org/10.1039/C6AY02733D>.
- Crossman, J., Hurley, R.R., Futter, M., Nizzetto, L., 2020. Transfer and transport of microplastics from biosolids to agricultural soils and the wider environment. *Sci. Total Environ.* 724, 138334 <https://doi.org/10.1016/j.scitotenv.2020.138334>.
- De Frond, H., Rubinovitz, R., Rochman, C.M., 2021. μ ATR-FTIR spectral libraries of plastic particles (FLOPP and FLOPP-e) for the analysis of microplastics. *Anal. Chem.* 93 (48), 15878–15885. <https://doi.org/10.1021/acs.analchem.1c02549>.
- Dekiff, J.H., Remy, D., Klasmeyer, J., Fries, E., 2014. Occurrence and spatial distribution of microplastics in sediments from Norderney. *Environ. Pollut.* 186, 248–256. <https://doi.org/10.1016/j.envpol.2013.11.019>.
- Dey, T., 2023. Microplastic pollutant detection by Surface Enhanced Raman Spectroscopy (SERS): a mini-review. *Nanotechnol. Environ. Eng.* 8 (1), 41–48. <https://doi.org/10.1007/s41204-022-00223-7>.
- Ding, L., Zhang, S., Wang, X., Yang, X., Zhang, C., Qi, Y., Guo, X., 2020. The occurrence and distribution characteristics of microplastics in the agricultural soils of Shaanxi Province, in north-western China. *Sci. Total Environ.* 720, 137525 <https://doi.org/10.1016/j.scitotenv.2020.137525>.
- Dümichen, E., Eisentraut, P., Bannick, C.G., Barthel, A.-K., Senz, R., Braun, U., 2017. Fast identification of microplastics in complex environmental samples by a thermal degradation method. *Chemosphere* 174, 572–584. <https://doi.org/10.1016/j.chemosphere.2017.02.010>.
- Edwards, M., Topp, E., Metcalfe, C.D., Li, H., Gottschall, N., Bolton, P., Curnoe, W., Payne, M., Beck, A., Kleywegt, S., Lapen, D.R., 2009. Pharmaceutical and personal care products in tile drainage following surface spreading and injection of dewatered municipal biosolids to an agricultural field. *Sci. Total Environ.* 407 (14), 4220–4230. <https://doi.org/10.1016/j.scitotenv.2009.02.028>.
- Elert, A.M., Becker, R., Dümichen, E., Eisentraut, P., Falkenhagen, J., Sturm, H., Braun, U., 2017. Comparison of different methods for MP detection: what can we learn from them, and why asking the right question before measurements matters? *Environ. Pollut.* 231, 1256–1264. <https://doi.org/10.1016/j.envpol.2017.08.074>.
- Fan, W., Qiu, C., Qu, Q., Hu, X., Mu, L., Gao, Z., Tang, X., 2023. Sources and identification of microplastics in soils. *Soil Environ. Health* 1 (2), 100019. <https://doi.org/10.1016/j.seh.2023.100019>.

- Felsing, S., Kochleus, C., Buchinger, S., Brennholt, N., Stock, F., Reifferscheid, G., 2018. A new approach in separating microplastics from environmental samples based on their electrostatic behavior. *Environ. Pollut.* 234, 20–28. <https://doi.org/10.1016/j.envpol.2017.11.013>.
- Foekema, E.M., De Gruijter, C., Mergia, M.T., van Franeker, J.A., Murk, A.J., Koelmans, A.A., 2013. Plastic in North Sea fish. *Environ. Sci. Technol.* 47 (15), 8818–8824. <https://doi.org/10.1021/es400931b>.
- Fraunholz, N., 2004. Separation of waste plastics by froth flotation—a review, part I. *Miner. Eng.* 17 (2), 261–268. <https://doi.org/10.1016/j.mineng.2003.10.028>.
- Frei, S., Piehl, S., Gilfedder, B.S., Löder, M.G.J., Krutzke, J., Wilhelm, L., Laforsch, C., 2019. Occurrence of microplastics in the hyporheic zone of rivers. *Sci. Rep.* 9 (1), 15256. <https://doi.org/10.1038/s41598-019-51741-5>.
- Fries, E., Dekiff, J.H., Willmeyer, J., Nuelle, M.-T., Ebert, M., Remy, D., 2013. Identification of polymer types and additives in marine microplastic particles using pyrolysis-GC/MS and scanning electron microscopy. *Environ. Sci. Process Impacts* 15 (10), 1949–1956. <https://doi.org/10.1039/C3EM00214D>.
- Gottschall, N., Topp, E., Edwards, M., Russell, P., Payne, M., Kleywegt, S., Curnoe, W., Lapen, D.R., 2010. Polybrominated diphenyl ethers, perfluorinated alkylated substances, and metals in tile drainage and groundwater following applications of municipal biosolids to agricultural fields. *Sci. Total Environ.* 408 (4), 873–883. <https://doi.org/10.1016/j.scitotenv.2009.10.063>.
- Gottschall, N., Topp, E., Metcalfe, C., Edwards, M., Payne, M., Kleywegt, S., Russell, P., Lapen, D.R., 2012. Pharmaceutical and personal care products in groundwater, subsurface drainage, soil, and wheat grain, following a high single application of municipal biosolids to a field. *Chemosphere* 87 (2), 194–203. <https://doi.org/10.1016/j.chemosphere.2011.12.018>.
- Graue, G., Kuniyasu, Y., Chien, M.-F., Inoue, C., 2022. Separation of microplastic from soil by centrifugation and its application to agricultural soil. *Chemosphere* 288, 132654. <https://doi.org/10.1016/j.chemosphere.2021.132654>.
- Grbic, J., Nguyen, B., Guo, E., You, J.B., Sinton, D., Rochman, C.M., 2019. Magnetic extraction of microplastics from environmental samples. *Environ. Sci. Technol. Lett.* 6 (2), 68–72. <https://doi.org/10.1021/acs.estlett.8b00671>.
- GUM, JCGM 100, 2008. Evaluation of Measurement Data — Guide to the Expression of Uncertainty in Measurement (GUM 1995 with Minor Corrections). https://www.bipm.org/documents/20126/2071204/JCGM_100_2008_E.pdf.
- Han, X., Lu, X., Vogt, R.D., 2019. An optimized density-based approach for extracting microplastics from soil and sediment samples. *Environ. Pollut.* 254, 113009. <https://doi.org/10.1016/j.envpol.2019.11.3009>.
- He, D., Luo, Y., Lu, S., Liu, M., Song, Y., Lei, L., 2018. Microplastics in soils: analytical methods, pollution characteristics and ecological risks. *TrAC Trends Anal. Chem.* 109, 163–172. <https://doi.org/10.1016/j.trac.2018.10.006>.
- He, D., Zhang, X., Hu, J., 2021. Methods for separating microplastics from complex solid matrices: comparative analysis. *J. Hazard. Mater.* 409, 124640. <https://doi.org/10.1016/j.jhazmat.2020.124640>.
- Herrera, A., Garrido-Amador, P., Martínez, I., Samper, M.D., López-Martínez, J., Gómez, M., Packard, T.T., 2018. Novel methodology to isolate microplastics from vegetal-rich samples. *Mar. Pollut. Bull.* 129 (1), 61–69. <https://doi.org/10.1016/j.marpolbul.2018.02.015>.
- Hintersteiner, I., Himmelsbach, M., Buchberger, W.W., 2015. Characterization and quantitation of polyolefin microplastics in personal-care products using high-temperature gel-permeation chromatography. *Anal. Bioanal. Chem.* 407 (4), 1253–1259. <https://doi.org/10.1007/s00216-014-8318-2>.
- Ho, W.-K., Law, J.C.-F., Zhang, T., Leung, K.S.-Y., 2020. Effects of weathering on the sorption behavior and toxicity of polystyrene microplastics in multi-solute systems. *Water Res.* 187, 116419. <https://doi.org/10.1016/j.watres.2020.116419>.
- Hu, B., 2014. Magnetic Density Separation of Polyolefin Wastes, ISBN 978-94-6169-526-0. <https://doi.org/10.4233/uid:0c3717fa-8000-4de0-a938-d65605bf2a96>.
- Hu, J., He, D., Zhang, X., Li, X., Chen, Y., Wei, G., Zhang, Y., Ok, Y.S., Luo, Y., 2022. National-scale distribution of micro(meso)plastics in farmland soils across China: implications for environmental impacts. *J. Hazard. Mater.* 424 (Part A), 127283. <https://doi.org/10.1016/j.jhazmat.2021.127283>.
- Hurler, R.R., Lusher, A.L., Olsen, M., Nizzetto, L., 2018. Validation of a method for extracting microplastics from complex, organic-rich, environmental matrices. *Environ. Sci. Technol.* 52 (13), 7409–7417. <https://doi.org/10.1021/acs.est.8b01517>.
- Imhof, H.K., Schmid, J., Niessner, R., Ivleva, N.P., Laforsch, C., 2012. A novel, highly efficient method for the separation and quantification of plastic particles in sediments of aquatic environments. *Limnol. Oceanogr. Methods* 10 (7), 524–537. <https://doi.org/10.4319/lom.2012.10.524>.
- Katsumi, N., Nagao, S., Okochi, H., 2022. Addition of polyvinyl pyrrolidone during density separation with sodium iodide solution improves recovery rate of small microplastics (20–150 μm) from soils and sediments. *Chemosphere* 307, 135730. <https://doi.org/10.1016/j.chemosphere.2022.135730>.
- Kawecki, D., Nowack, B., 2019. Polymer-specific modeling of the environmental emissions of seven commodity plastics as macro- and microplastics. *Environ. Sci. Technol.* 53 (16), 9664–9676. <https://doi.org/10.1021/acs.est.9b02900>.
- Kedzierski, M., Le Tilly, V., Bourseau, P., Bellegou, H., César, G., Sire, O., Bruzaud, S., 2016. Microplastics elutriation from sandy sediments: a granulometric approach. *Mar. Pollut. Bull.* 107 (1), 315–323. <https://doi.org/10.1016/j.marpolbul.2016.03.041>.
- Kim, Y.-N., Yoon, J.-H., Kim, K.-H.J., 2020. Microplastic contamination in soil environment – a review. *Soil Sci. Annu.* 71 (4), 300–308. <https://doi.org/10.37501/soilsa/131646>.
- Kononov, A., Hishida, M., Suzuki, K., Harada, N., 2022. Microplastic extraction from agricultural soils using canola oil and unsaturated sodium chloride solution and evaluation by incineration method. *Soil Syst.* 6 (2), 54. <https://doi.org/10.3390/soilsystems6020054>.
- Kopatz, V., Wen, K., Kovács, T., Keimowitz, A.S., Pichler, V., Widder, J., Vethaak, A.D., Hollóczki, O., Kenner, L., 2023. Micro- and nanoplastics breach the blood-brain barrier (BBB): biomolecular corona's role revealed. *Nanomaterials* 13 (8), 1404. <https://doi.org/10.3390/nano13081404>.
- La Nasa, J., Biale, G., Mattonai, M., Modugno, F., 2021. Microwave-assisted solvent extraction and double-shot analytical pyrolysis for the qualitative-quantitative of plasticizers and microplastics in beach sand samples. *J. Hazard. Mater.* 401, 123287. <https://doi.org/10.1016/j.jhazmat.2020.123287>.
- Lapen, D.R., Topp, E., Metcalfe, C.D., Li, H., Edwards, M., Gottschall, N., Bolton, P., Curnoe, W., Payne, M., Beck, A., 2008. Pharmaceutical and personal care products in tile drainage following land application of municipal biosolids. *Sci. Total Environ.* 399 (1), 50–65. <https://doi.org/10.1016/j.scitotenv.2008.02.025>.
- Lechthaler, S., Hildebrandt, L., Stauch, G., Schüttrumpf, H., 2020. Canola oil extraction in conjunction with a plastic free separation unit optimises microplastics monitoring in water and sediment. *Anal. Methods* 12 (42), 5128–5139. <https://doi.org/10.1039/D0AY01574A>.
- Li, Q., Wu, J., Zhao, X., Gu, X., Ji, R., 2019. Separation and identification of microplastics from soil and sewage sludge. *Environ. Pollut.* 254, 113076. <https://doi.org/10.1016/j.envpol.2019.11.3076>.
- Li, L., Li, S., Xu, Y., Ren, L., Yang, L., Liu, X., Dai, Y., Zhao, J., Yue, T., 2023. Distinguishing the nanoplastic-cell membrane interface by polymer type and aging properties: translocation, transformation and perturbation. *Environ. Sci. Nano* 10 (2), 440–453. <https://doi.org/10.1039/D2EN00800A>.
- Liu, X., Sang, Y., Yin, H., Lin, A., Guo, Z., Liu, Z., 2018. Progress in the mechanism and kinetics of Fenton reaction. *MOJ Eco. Environ. Sci.* 3 (1), 00060. <https://doi.org/10.15406/mojes.2018.03.00060>.
- Löder, M.G.J., Kuczera, M., Mintenig, S., Lorenz, C., Gerdts, G., 2015. Focal plane array detector-based micro-Fourier-transform infrared imaging for the analysis of microplastics in environmental samples. *Environ. Chem.* 12 (5), 563–581. <https://doi.org/10.1071/EN14205>.
- Maaß, S., Daphi, D., Lehmann, A., Rillig, M.C., 2017. Transport of microplastics by two collembolan species. *Environ. Pollut.* 225, 456–459. <https://doi.org/10.1016/j.envpol.2017.03.009>.
- Maes, T., Jessop, R., Wellner, N., Haupt, K., Mayes, A.G., 2017. A rapid-screening approach to detect and quantify microplastics based on fluorescent tagging with Nile Red. *Sci. Rep.* 7 (1), 44501. <https://doi.org/10.1038/srep44501>.
- Mansa, R., Zou, S., 2021. Thermogravimetric analysis of microplastics: a mini review. *Environ. Adv.* 5, 100117. <https://doi.org/10.1016/j.envadv.2021.100117>.
- Mattsson, K., Ekstrand, E., Granberg, M., Hasselöv, M., Magnusson, K., 2022. Comparison of pre-treatment methods and heavy density liquids to optimize microplastic extraction from natural marine sediments. *Sci. Rep.* 12 (1), 15459. <https://doi.org/10.1038/s41598-022-19623-5>.
- Mbachu, O., Jenkins, G., Pratt, C., Kaporaju, P., 2021. Enzymatic purification of microplastics in soil. *MethodsX* 8, 101254. <https://doi.org/10.1016/j.mex.2021.101254>.
- Möller, J.N., Heisel, I., Satzger, A., Vizsolyi, E.C., Oster, S.D.J., Agarwal, S., Laforsch, C., Löder, M.G.J., 2022. Tackling the challenge of extracting microplastics from soils: a protocol to purify soil samples for spectroscopic analysis. *Environ. Toxicol. Chem.* 41 (4), 844–857. <https://doi.org/10.1002/etc.5024>.
- Munno, K., De Frond, H., O'Donnell, B., Rochman, C.M., 2020. Increasing the accessibility for characterizing microplastics: introducing new application-based and spectral libraries of plastic particles (SLOPP and SLOPP-E). *Anal. Chem.* 92 (3), 2443–2451. <https://doi.org/10.1021/acs.analchem.9b03626>.
- Naderi Beni, N., Karimifard, S., Gilley, J., Messer, T., Schmidt, A., Bartel-Hunt, S., 2023. Higher concentrations of microplastics in runoff from biosolid-amended croplands than manure-amended croplands. *Commun. Earth Environ.* 4 (1), 42. <https://doi.org/10.1038/s43247-023-00691-y>.
- Nakajima, R., Tsuchiya, M., Lindsay, D.J., Kitahashi, T., Fujikura, K., Fukushima, T., 2019. A new small device made of glass for separating microplastics from marine and freshwater sediments. *PeerJ* 7, e7915. <https://doi.org/10.7717/peerj.7915>.
- Nava, V., Frezzotti, M.L., Leoni, B., 2021. Raman spectroscopy for the analysis of microplastics in aquatic systems. *Appl. Spectrosc.* 75 (11), 1341–1357. <https://doi.org/10.1177/00037028211043119>.
- Nizzetto, L., Futter, M., Langaas, S., 2016. Are agricultural soils dumps for microplastics of urban origin? *Environ. Sci. Technol.* 50 (20), 10777–10779. <https://doi.org/10.1021/acs.est.6b04140>.
- Nuelle, M.-T., Dekiff, J.H., Remy, D., Fries, E., 2014. A new analytical approach for monitoring microplastics in marine sediments. *Environ. Pollut.* 184, 161–169. <https://doi.org/10.1016/j.envpol.2013.07.027>.
- Okoffo, E.D., Ribeiro, F., O'Brien, J.W., O'Brien, S., Tschärke, B.J., Gallen, M., Samanipour, S., Mueller, J.F., Thomas, K.V., 2020. Identification and quantification of selected plastics in biosolids by pressurized liquid extraction combined with double-shot pyrolysis gas chromatography-mass spectrometry. *Sci. Total Environ.* 715, 136924. <https://doi.org/10.1016/j.scitotenv.2020.136924>.
- Palacios-Mateo, C., Meng, K., Legaz-Pol, L., Steen Redeker, E., Huerta-Lwanga, E., Blank, L.M., 2023. Enzymes for microplastic-free agricultural soils. *Ecotoxicol. Environ. Saf.* 258, 114982. <https://doi.org/10.1016/j.ecoenv.2023.114982>.
- Qiu, Q., Tan, Z., Wang, J., Peng, J., Li, M., Zhan, Z., 2016. Extraction, enumeration and identification methods for monitoring microplastics in the environment. *Estuar. Coast. Shelf Sci.* 176, 102–109. <https://doi.org/10.1016/j.ecss.2016.04.012>.
- Radford, F., Zapata-Restrepo, L.M., Horton, A.A., Hudson, M.D., Shaw, P.J., Williams, I.D., 2021. Developing a systematic method for extraction of microplastics in soils. *Anal. Methods* 13 (14), 1695–1705. <https://doi.org/10.1039/D0AY02086A>.

- Radford, F., Horton, A., Hudson, M., Shaw, P., Williams, I., 2023. Agricultural soils and microplastics: are biosolids the problem? *Front. Soil Sci.* 2, 941837 <https://doi.org/10.3389/fsoil.2022.941837>.
- Renner, G., Schmidt, T.C., Schram, J., 2017. Chapter 4 - characterization and quantification of microplastics by infrared spectroscopy. In: Rocha-Santos, T.A.P., Duarte, A.C. (Eds.), *Comprehensive Analytical Chemistry*, vol. 75. Elsevier, pp. 67–118. <https://doi.org/10.1016/bs.coac.2016.10.006>.
- Rhein, F., Scholl, F., Nirschl, H., 2019. Magnetic seeded filtration for the separation of fine polymer particles from dilute suspensions: microplastics. *Chem. Eng. Sci.* 207, 1278–1287. <https://doi.org/10.1016/j.ces.2019.07.052>.
- Rillig, M.C., Ziersch, L., Hempel, S., 2017. Microplastic transport in soil by earthworms. *Sci. Rep.* 7 (1), 1362. <https://doi.org/10.1038/s41598-017-01594-7>.
- Silveira, A.V.M., Cella, M., Tanabe, E.H., Bertuol, D.A., 2018. Application of tribo-electrostatic separation in the recycling of plastic wastes. *Process. Saf. Environ. Prot.* 114, 219–228. <https://doi.org/10.1016/j.psep.2017.12.019>.
- Sivarajah, B., Lapen, D.R., Gewurtz, S.B., Smyth, S.A., Provencher, J.F., Vermaire, J.C., 2023. How many microplastic particles are present in Canadian biosolids? *J. Environ. Qual.* 52, 1037–1048. <https://doi.org/10.1002/jeq2.20497>.
- Sobhani, Z., Luo, Y., Gibson, C.T., Tang, Y., Naidu, R., Megharaj, M., Fang, C., 2021. Collecting microplastics in gardens: case study (i) of soil. *Front. Environ. Sci.* 9, 739775 <https://doi.org/10.3389/fenvs.2021.739775>.
- Toto, B., Refosco, A., Dierkes, J., Kögel, T., 2023. Efficient extraction of small microplastic particles from rat feed and feces for quantification. *Heliyon* 9 (1), e12811. <https://doi.org/10.1016/j.heliyon.2023.e12811>.
- Van Cauwenbergh, L., Devriese, L., Galgani, F., Robbins, J., Janssen, C.R., 2015. Microplastics in sediments: a review of techniques, occurrence and effects. *Mar. Environ. Res.* 111, 5–17. <https://doi.org/10.1016/j.marenvres.2015.06.007>.
- Wang, Z., Taylor, S.E., Sharma, P., Flury, M., 2018. Poor extraction efficiencies of polystyrene nano- and microplastics from biosolids and soil. *PLoS One* 13 (11), e0208009. <https://doi.org/10.1371/journal.pone.0208009>.
- Wang, W., Zhang, J., Qiu, Z., Cui, Z., Li, N., Li, X., Wang, Y., Zhang, H., Zhao, C., 2022. Effects of polyethylene microplastics on cell membranes: a combined study of experiments and molecular dynamics simulations. *J. Hazard. Mater.* 429, 128323 <https://doi.org/10.1016/j.jhazmat.2022.128323>.
- Wick, L.Y., Remer, R., Würz, B., Reichenbach, J., Braun, S., Schäfer, F., Harms, H., 2007. Effect of fungal hyphae on the access of bacteria to phenanthrene in soil. *Environ. Sci. Technol.* 41 (2), 500–505. <https://doi.org/10.1021/es061407s>.
- Yang, J., Li, L., Li, R., Xu, L., Shen, Y., Li, S., Tu, C., Wu, L., Christie, P., Luo, Y., 2021. Microplastics in an agricultural soil following repeated application of three types of sewage sludge: a field study. *Environ. Pollut.* 289, 117943 <https://doi.org/10.1016/j.envpol.2021.117943>.
- Yu, J., Wang, P., Ni, F., Cizdziel, J., Wu, D., Zhao, Q., Zhou, Y., 2019. Characterization of microplastics in environment by thermal gravimetric analysis coupled with Fourier transform infrared spectroscopy. *Mar. Pollut. Bull.* 145, 153–160. <https://doi.org/10.1016/j.marpolbul.2019.05.037>.
- Zhang, F., Tang, X., Tong, A., Wang, B., Wang, J., 2020. An automatic baseline correction method based on the penalized least squares method. *Sensors* 20 (7), 2015. <https://doi.org/10.3390/s20072015>.